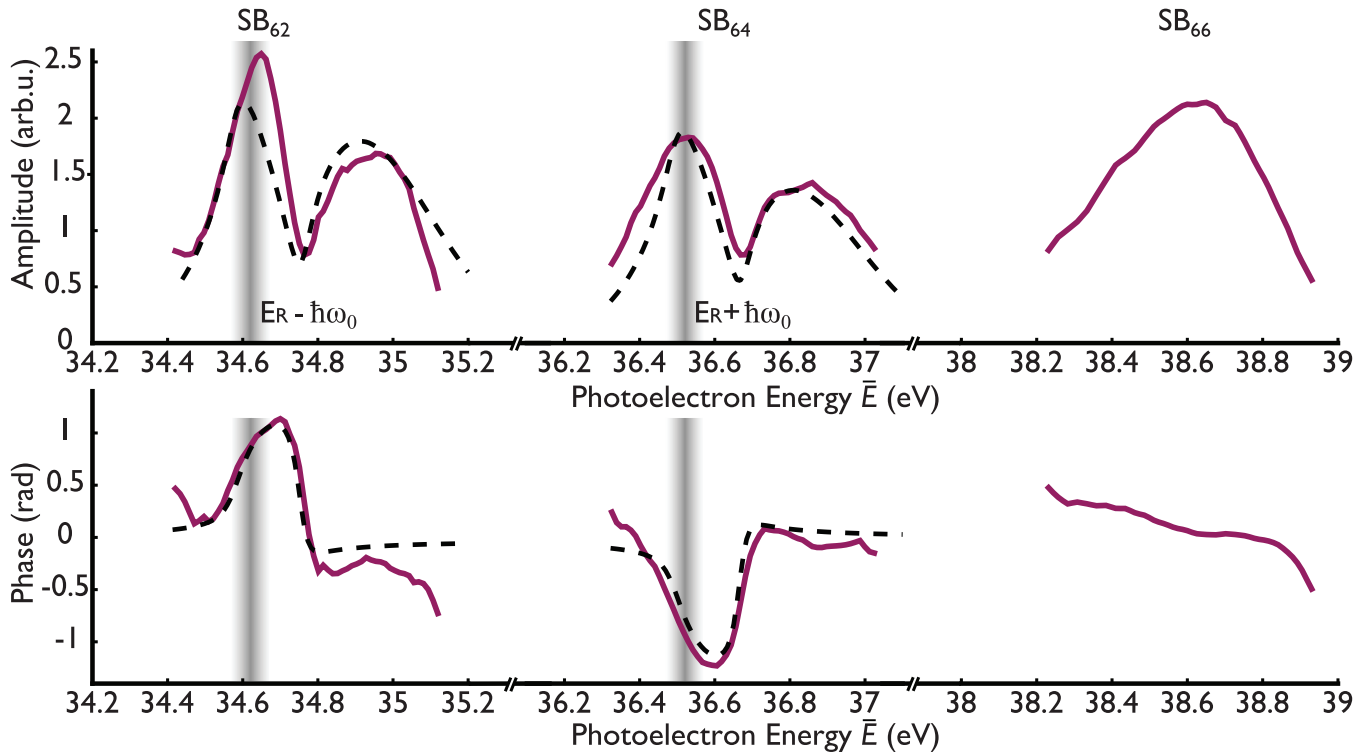

Fig. 2. Resonant EWP in the spectral domain. Upper and lower panels respectively show spectral amplitude and phase of the $2\omega_0$ component of SB_{62} (left), SB_{64} (center), and SB_{66} (right) from the spectrograms in Fig. 1, B and C. The phase origin is set to 0 by removing the linear variation due to the ionizing harmonic radiation (attochirp) (*30*). The experimental data (purple curves) show very good agreement with the simulations (dashed black lines). The resonance position shifted by one MIR photon is indicated in gray. The measured spectral amplitudes and phases of the resonant SB_{62} and SB_{64} are easily related to the amplitude $|A_R(E)|$ and phase $\eta_{scat}(E)$ of the resonant one-photon EWP (see Eq. 1). The main limitation comes from the current spectrometer resolution (in our conditions, a relative resolution of ~1.9% resulting in a width of ~190 meV at 10 eV) that broadens the resonant peak and its phase variations. The nonresonant SB_{66} exhibits a Gaussian amplitude (which mostly reflects the ionizing XUV spectral profile) and a smooth close-to-linear phase. This provides a temporal reference for the ionization dynamics.

origin—given by the maximum of the Fourier transform of the nonresonant SB_{66} (*25*)—followed by a deep minimum around 4 fs and then a revival with a decay within ~10 fs. The presence of a fast phase jump (~2 rad within ~2 fs) at the position of the minimum indicates that it results from a destructive interference between two wave packet components, the origin of which is detailed below.

To benchmark the measured data, we theoretically investigated the multicolor XUV + MIR ionization of He in the vicinity of the 2s2p resonance. Fully correlated ab initio time-dependent calculations (*22*) were used to validate an analytical model of the two-photon transitions accounting for the actual pulses' bandwidths (*23*). The simulated photoelectron spectrogram, taking into account the spectrometer resolution, remarkably reproduces the structured shape of the resonant sidebands as well as the dephasing between their two components (Fig. 1C). The analysis of the $2\omega_0$ oscillations of SB_{62} and SB_{64} gives spectral phase variations in excellent agreement with the experimental data (Fig. 2). The temporal profile $\tilde{A}_R(t)$ obtained by Fourier transform (Fig. 3) is also well reproduced, with a smaller revival but a similar decay time of ~10 fs. This reduced effective lifetime is a direct consequence of the finite spectrometer resolution. When the latter is assumed infinite, the time profile has the same behavior at short times but a longer decay, corresponding to the 17-fs lifetime of the resonance. Analytical calculations show that in our conditions, the reconstructed EWP does mirror the one-photon resonant EWP (*25*). These findings confirm that, except for a faster decay of the long-term tail due to our current electron spectrometer resolution, the essential physics of the early time frame of EWP creation is directly accessed from purely experimental data.

To further highlight the insight provided by this experimental technique, we undertook an in-depth analysis of the measured EWP characteristics in terms of Fano's formalism for autoionization (*14*). Resonant ionization can be described as the interference between two distinct paths: (i) the direct transition to the continuum, and (ii) the resonant transition through the doubly excited state that eventually decays in the continuum through configuration interaction within the resonance lifetime (Fig. 3B). The normalized total transition amplitude can then be written as the coherent sum of two contributions, a constant background term and a Breit-Wigner amplitude for the resonance:

$$R(E) = \frac{\varepsilon + q}{\varepsilon + i} = 1 + \frac{q - i}{\varepsilon + i} \qquad (3)$$

where $\varepsilon = 2(E - E_R)/\Gamma$ is the reduced energy detuning from the resonance at energy E_R, in units of its half width $\Gamma/2$. The Fano parameter q [−2.77 for the He(2s2p) resonance (*16*)] measures the relative weight of the two paths. Their interference leads to the well-known asymmetric Fano line shape $|R(E)|^2$ and to the resonant scattering phase: $\eta_{scat}(E) = \arg R(E) = \text{atan}(\varepsilon) + \pi/2 - \pi\Theta(\varepsilon + q)$, where Θ is the Heaviside function. This phase is experimentally accessed here (Fig. 2).

The spectral amplitude of an EWP created by Gaussian harmonic excitation $H(E)$ is given by $R(E)H(E)$. Its temporal counterpart is $\tilde{A}_R(t) = [\tilde{R} * \tilde{H}](t)$, where $\tilde{R}(t)$ and $\tilde{H}(t)$ are Fourier transforms of the spectral amplitudes, in particular

$$\tilde{R}(t) = \delta(t) - i\frac{\Gamma}{2\hbar}(q - i)\exp\left[-\left(\frac{iE_R}{\hbar} + \frac{\Gamma}{2\hbar}\right)t\right]\Theta(t) \qquad (4)$$